www.czasopisma.pan.pl PAN POLSKA AKADEMIA NAUK www.journals.pan.pl

Arch. Metall. Mater., Vol. 61 (2016), No 4, p. 1793–1794

DOI: 10.1515/amm-2016-0290

R. KACZYŃSKI*,#, G. ROGOWSKI*, B. HOŚCIŁO*

THE USE OF INSTRUMENTAL HARDNESS MEASUREMENTS IN DETERMINING STRESSES IN THE ELASTIC ELEMENTS OF A MANIPULATOR FOR SERVICING WATER AND SEWAGE NETWORKS

The paper presents the design of a manipulator for servicing the elements of water and sewage infrastructure, in particular for installation and dismantling of pressure transducers without the need for earthmoving. To build this device the resilient elements, cold shaped, responsible for centering the manipulator in the technical tube were used. In their construction a method was applied of estimating the value of residual stresses in the cold shaped material, based on measurements of instrumental hardness. The experimental verification of numerical simulation of instrumental hardness measurements of flat springs made of 1.1274 steel is described.

1. Introduction

Monitoring the water distribution systems and sewerage systems is an essential element of effective management of the existing municipal infrastructure operation. Service works related to the replacement, maintenance and periodic inspection of the measuring and control elements located directly on the pipeline are costly and challenging engineering tasks. This is largely due to the placement of pipelines usually under the traffic lanes, roads, sidewalks or near them. To access the pressure transducers that require periodic inspections earthworks were conducted so far and the section of road was temporarily closed for use. The next stage that generated significant costs was to restore the roadway to its previous state, to repair the road, sidewalk, etc. Even a slight decrease in the cost of such work is highly reasonable. To meet the suggestions of companies providing service of pipeline monitoring devices the prototype was constructed and built of a manipulator for servicing pressure transducers without the need for excavation work during their replacement.

One of the manipulator construction elements are resilient elements used to capture the dismantled transducer and center the device in the technical pipe. They are made from a strip of 1.1274 spring steel for cold shaping. Such treatment introduces considerable internal stresses that lead to premature cracking of the element. An important issue seems to be determining the level of residual stresses in relation to the ultimate strength of the material. To determine them the measurement of instrumental micro-hardness was used, described inter alia in papers [1,2] and its use for determining the residual strain in the material [3] and based on Oliver-Pharr model [4,5]. Numerical simulations of the phenomenon were performed using the FEM (finite element method), the results were verified experimentally by measuring the instrumental micro-hardness of the material before cold shaping and after it.

2. Manipulator for trenchless servicing of pressure transducers

Manipulator for trenchless servicing of the infrastructure elements of water and sewage networks is a unique device which enables carrying out inspection work and activities related to the installation and dismantling of such elements in pipelines with an internal diameter of 40 to 50 mm. It is a device composed of two modules: a module providing an anchor (immobilization) of the manipulator in a technical pipe A and the module responsible for dismantling and installation of the pressure transducer B, Fig. 1. The modules are interconnected by means of a susceptible clutch C that allows the manipulator operation in the curved pieces on a pipeline.

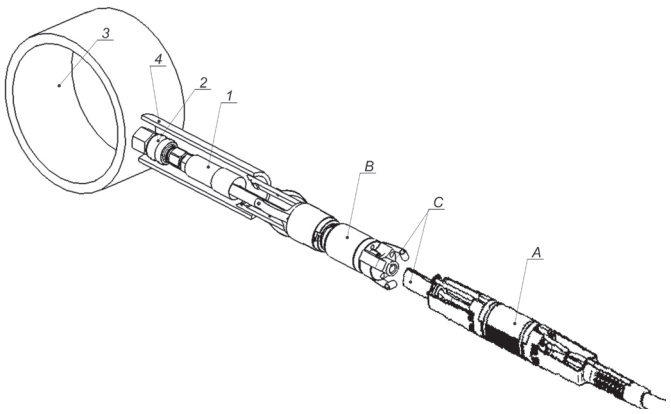

Fig. 1. Manipulator for trenchless servicing of the infrastructure elements of water and sewage networks: A – block module of the manipulator, B – module for dismantling and installation of a transducer, C – clutch, 1 – transducer, 2 – hydraulic quick coupler, 3 – pipeline, 4 – technical pipe

* BIALYSTOK UNIVERSITY OF TECHNOLOGY, FACULTY OF MECHANICAL ENGINEERING, 45C WIEJSKA 45 STR., 15-351 BIALYSTOK, POLAND

Corresponding author: r.kaczynski@pb.edu.pl

Generally, the device is used for maintenance works which include above all the exchange of the pressure transducer 1, fixed by means of a hydraulic quick coupler 2 in the outer surface of the water pipeline 3. The manipulator moves in a technical pipe of an internal diameter from 40 to 50mm (Fig. 1).

Manipulator for trenchless servicing of the infrastructure elements of water and sewage networks is supplied with compressed air at 0,8 MPa.

In the module for installation and dismantling the pressure transducer the supply medium is fed through a pneumatic quick coupler 5 (Fig. 2) to a longitudinal actuator composed of a piston rod 6 with seals 7, 8, 9 and 10 and return spring 11. These elements are housed in a cylinder 12 closed with covers 13 and 14. A through hole of the plunger 2 allows the actuator to translate the signal line of the transducer 1. The through hole inside the piston 2 makes it possible to translate by the actuator the transducer signal wire 1. On the side of compressed air supply, a flexible clutch 15 is attached to the actuator connecting the actuator module providing a longitudinal immobilization of the manipulator in the technical pipe 4. On the opposite side of the actuator, on the piston rod a bayonet coupling 16 is attached with locking screws 17. These screws act as locks of removal gripper for dismantling 18 and the gripper for installation 19. Flat springs 20 and 21 are intended to center the gripper and the actuator on the symmetry axis in the technical pipe 4. The pressure transducer 1 is mounted and centered in the gripper with the use of a compliant faucet 22 or 23. The manipulator grippers are equipped with a micro camera 24 which allows monitoring the processes of installation and dismantling of the transducer and its correct mounting in a slot of the water pipe coupler.

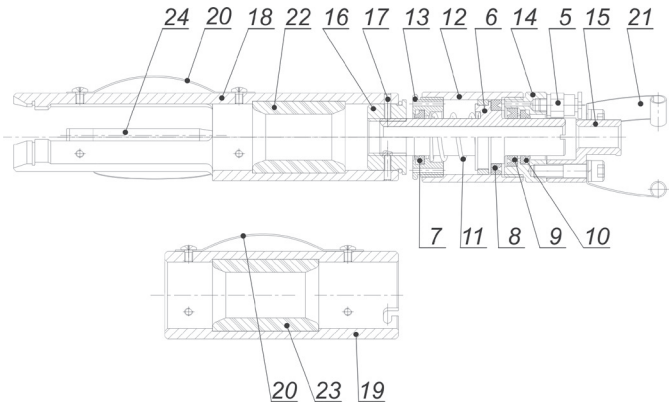

Fig. 2. Scheme of the module for installation and dismantling the pressure transducer: 5 – pneumatic quick coupler, 6 – piston rod, 7-10 – sealants, 11 – spring, 12 – cylinder, 13-14 – cylinder covers, 15 – element of the flexible clutch, 16 – bayonet coupling, 17 – locking screws, 18 – dismantling gripper, 19 – installation gripper, 20-21 – flat springs, 22-23 – compliant faucet, 24 – inspection micro-camera

In order to ensure the correct position of the manipulator relative to the pressure transducer and the centering device inside the technical pipe the spring elements 20 and 21 were used (FIG. 2) made of spring steel 1.1274 in the process of cold shaping. The material used was a strip 12.5 mm wide and 0.2 mm thick, cold-rolled, hardened and tempered. The formation of such material introduces significant residual stresses and can cause cracking of parts during operation. Therefore it becomes important to determine the level of residual stresses introduced in the process of cold shaping.

3. Methodology of testing the hardness

Authors of the work [3,6] present the method for defining residual stresses based on the values obtained in the course of determining instrumental hardness. Instrumental hardness is defined as the relation of the intender maximum loading force and the surface of imprint on unloading. This area is calculated based on the size of immersion. Devices used for such measurements record continuously the size of immersion and the strength of impact on the indenter during loading and unloading. On this basis a P-h diagram is created, from which with the use of Oliver Pharr model [4], certain properties of the material can be determined.

Residual stresses, according to the described method [3], may be determined based on the difference between the values determined for reference material (free of plastic residual stresses) and the corresponding values read from the P-h curve of the material with elastic residual stresses. To determine the residual stress necessary are: the P0-h0 curve of the measure in a zone free of residual stress and the P-h curve of the same material, but at the location of stresses. An example curve for the test material before the cold treatment is shown in Fig. 3.

To determine the residual stress the tests were carried out in two cycles at a constant size of the maximum immersion, while recording the impact of material on the indenter. The speed of immersion and withdrawal of the indenter was 2500 nm / min, the maximum penetration depth of 4000 nm.

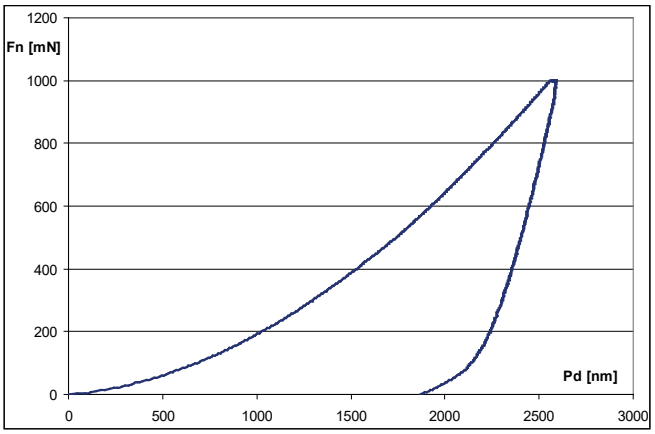

Fig. 3. Curve *P-h* received while measuring the hardness HV 0.1 of 1.1274 steel as delivered

Properties of the studied material are shown in Table 1. Testing feeler precision hardened and tempered High Carbon Steel 1.1274 of 12.7 mm wide and 0.2 mm thick.

TABLE 1

Properties of steel 1.1274

Rm	Re	HV0,1	E	n
MPa	MPa	Vickers	GPa	-
2278	2075	638	220.9	0.3

In the samples additional residual stresses were introduced through permanent plastic strain resulting from bending the strips at an angle of 30º on the radius of 1 mm. Measurements of so strained material hardness were made on the inside (compressive stresses introduced) and on the outer side (tensile residual stresses).

4. Numerical modeling

An attempt was made to model the issues of Vikers intender immersion in elastic-plastic sheet material with the use of finite element method. In Vickers indenter modeling the following were adopted for the diamond in accordance with the manufacturer's certificate E=1141GPa, $\nu = 0.07$, $\alpha = 136^{\circ}$, rounding radius tip 100 nm.

FIG. 4a presents the adopted size and boundary conditions of the three-dimensional model. Due to the large dimensions of the sheet in comparison to the indenter a roll of dimensions shown in Fig. 4a was adopted as its geometry. Using the symmetry of the issue one quarter of geometry was considered by applying appropriate conditions on the surfaces of symmetry.

FIG. 4b shows a finite element mesh. The mesh was concentrated in the area of the expected large gradients of stresses and strains.

In the numerical analysis the intender material due to its high rigidity of was taken as a ideally rigid material. The material properties of the tested sheet were taken as the elastic-plastic with a small linear hardening. Since in the three-dimensional, contact numerical analysis large plastic strain areas are expected a solver generally used for dynamic calculations (Explicit solver) was selected in order to obtain the solution convergence. By appropriate choice of the speed and mass of both elements in the analysis quasi-static conditions were obtained thereby eliminating the significance of dynamic forces and kinetic energy.

The analysis was based on application of displacement boundary conditions to perfectly rigid indenter, which allowed for further stabilization of the solution convergence. The displacement of the block by the experimentally measured value (2550 nm) gave rise to a reaction force, which value as a function of time is shown in Figure 5. On the graph there is interference characteristic of quasi-static analysis. In order to minimize them the analysis time should be lengthened, but this would make the calculations longer. The intended total analysis

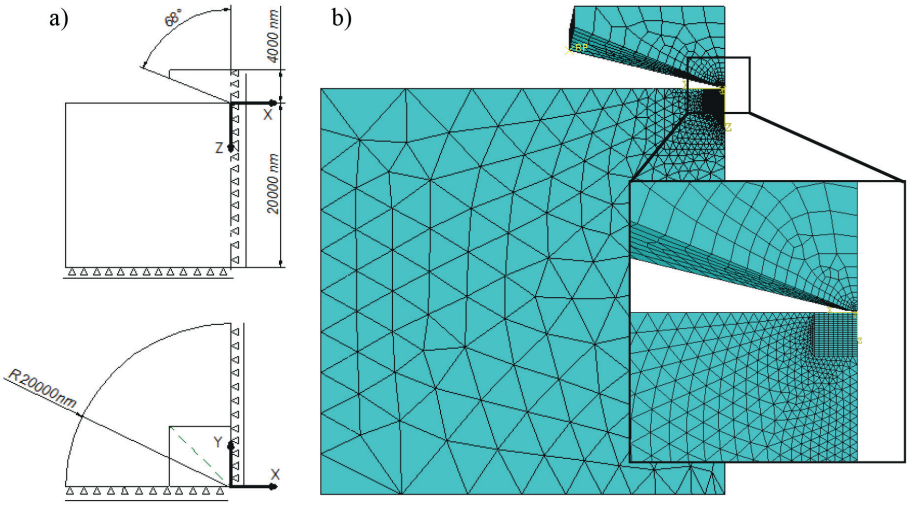

Fig. 4. Model MES: a – boundary conditions, b – finite element mesh

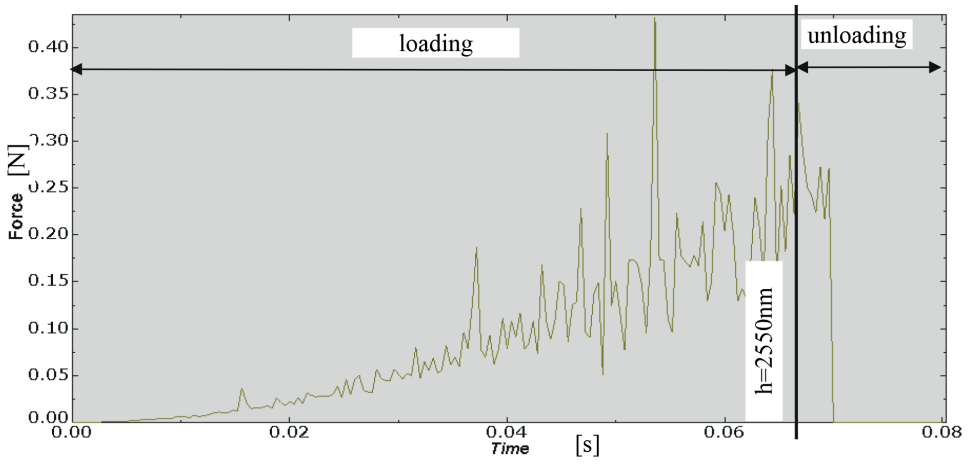

Fig. 5. FEM results of force enforcing the Vickers indenter immersion in the quasi-static analysis

time was 0.08s. For 0.07s the indenter was being pressed and the remaining 0.01s it was being withdrawn. The modeled speed of immersing the indenter into the sheet material did not exceed 1.5% elastic wave speed estimated from the ratio of $c = \sqrt{(E / q)}$, which allowed to maintain quasi-static conditions.

Figure 6 shows the results of numerical calculations of displacements in the Z axis direction on the upper surface of the sample. A square shaped clear imprint of the indenter is visible.

Fig. 7 presents the maps of normal stresses loading in a direction perpendicular to the upper surface of the sheet at the time of maximum displacement of the indenter and after its withdrawal.

Similar results are presented on Fig. 8 for reduced stresses by von Mises.

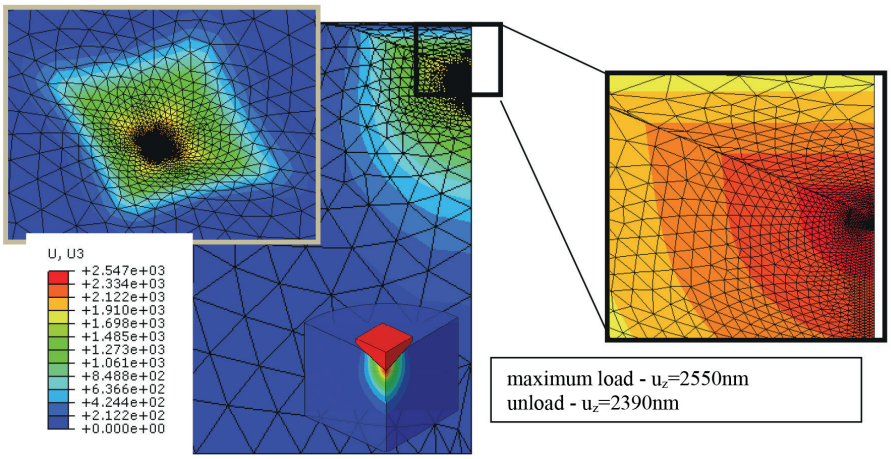

Fig. 6. Displacements of the material on the sheet surface u_z [nm] with maximum immersion of the intender

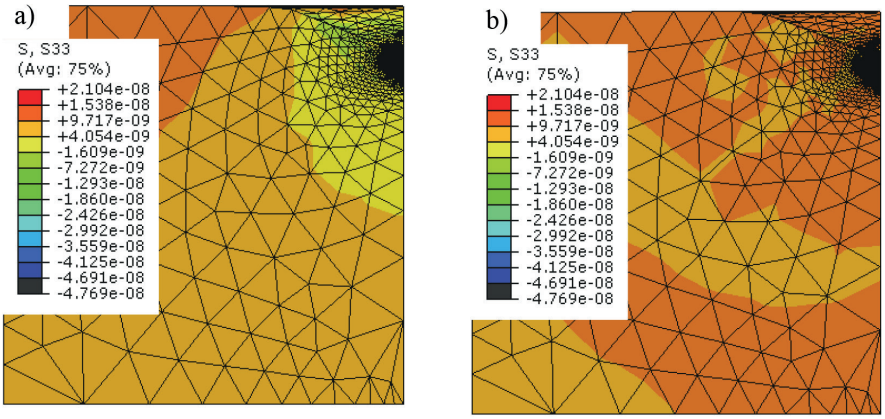

Fig. 7. Distribution of normal stress to the surface of the sheet σ_z [N/nm^2] a- maximum immersion of the intender, b – after unloading

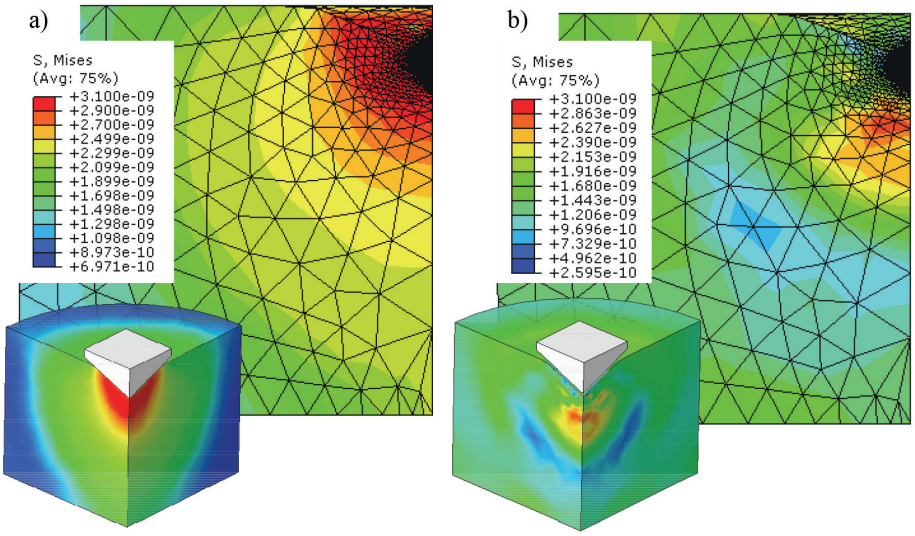

Fig. 8. Distribution of reduced stress σ_{zred} [N/nm^2] a) maximum immersion of the intender b – after unloading

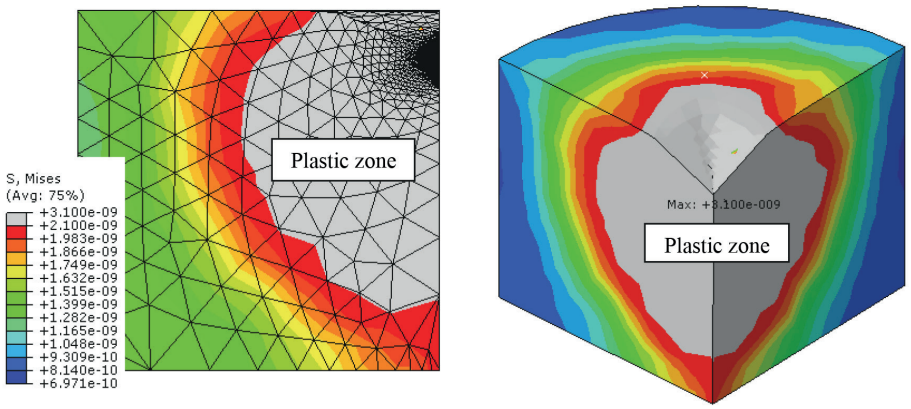

Fig. 9. Distribution of reduced stress σ_{mises} [N/nm^2] – maximum immersion of the intender – grey color indicates the zone of plastic strain

Fig. 9 shows a plastic strain zone of the sheet material extending in the depth. As seen from the presented results the depth of plastic strain occurrence is more than five times the penetration depth

5. Results and discussion

Fig. 10 shows the recorded curves respectively for the material before cold-forming - in the condition of delivery and after permanent deformation. Size F corresponds to the force opposing the indenter immersion recorded during the test. During the carrying out of the second load cycle there were clear differences visible between the values for not deformed sample and measurements on the compression and tension sides. On this basis, the sign of residual stresses in the case of unknown history samples can be specified

Tab. 2 summarizes the obtained values of selected parameters determined by measuring the instrumental hardness. They are important for residual stress analysis. Simultaneously, tensile residual stresses have a greater impact on the result of hardness measurement in comparison to compressive stress. The maximum indentation force varied from -0.3% with compressive stress to 7.6% with tensile stresses in comparison to the virgin material.

TABLE 2

Chosen characteristic average values calculated on the basis of the instrumental hardness measurement of 1.1274 steel

	Indentation hardness HIT	Vickers hardness HV	Maximum test force Fm	Contact stiffness S	Maximum indentation depth h_m	Plane strain modulus E*
	MPa	Vickers	mN	mN/nm	nm	GPa
Virgin material	6330.724	597.531	2174.097	3.864	4000	217.167
With tensile residual stress	6090.513	574.859	2008.156	2.524	4000	142.245
With compressive residual stress	6379.959	602.178	2179.766	3.873	4000	218.874

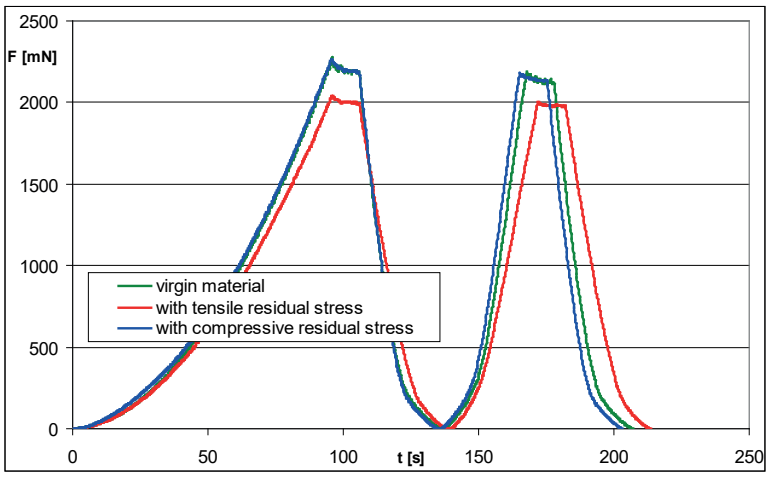

Fig. 10. Cycles realized during the instrumental hardness measurement of the material in the condition of delivery and after the introduction of residual stresses.

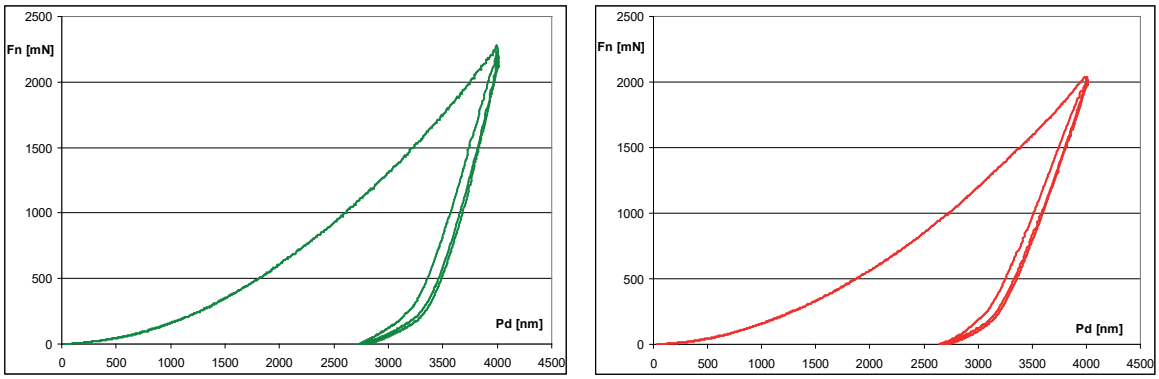

Fig. 11. Measurement of instrumental hardness curve P_0-h_0: a – in the zone free of residual stress, b – i.n the zone with tensile stresses

Fig. 11a illustrates the P0-h0 curves determined during the hardness measurement of the virgin material and Fig. 11b the measurement on the deformed side. A decrease of pressing resistance forces is visible with a constant, in both cases, depth of penetration. Contact stiffness of the deformed material also changes. On this basis the character of residual stresses can already be assumed, but their value is difficult to determine. This may be done indirectly on the basis of additional numerical analysis by introducing the initial conditions to the model of deformed material, in the form of negative or positive normal stress, in a direction parallel to the surface of the material. Selection of the appropriate value of these stresses in the process of inverse analysis, matching the curve P0-h0 obtained in numerical way to P0-h0 curve obtained experimentally, will determine the value of internal stresses

Because of the high non-linearity, both material and geometric, the achieved convergence of the iterative numerical solution is very difficult. As shown in this paper, it is possible to solve the problem using solvers dedicated for quick non-linear calculations (Explicit solvers) proposed in most commercial FEM software. The additional possibility of introducing the models of material destruction increases their competitiveness in comparison to standard solvers (Implicit solvers) providing the possibility of better matching the numerical and experimental results in nonlinear problems.

However, because of the issues of dynamics, the creation of smooth charts defining the forces that result from the contact of modeled objects, becomes a problem and hinders their later analysis. This problem can be solved by decreasing the strain rate which, however, significantly affects the calculation time. Reaching a compromise between the time of calculation and obtaining satisfactory results of quasi-static analysis requires a series of numerical tests. Additional use of appropriate approximation procedures would probably facilitate faster achieving the compliance of experimental and numerical tests results.

REFERENCES

[1] M.R.VanLandingham, Review of Instrumented Indentation. Journal of Research of the National Institute of Standards and Technology **108**, 249-265 (2003).

[2] Standard Test Method for Microindentation Hardness of Materials, E 384 – 05a C.F.R. (2005).

[3] S. Suresh, A.E. Giannakopoulos, A new method for estimating residual stresses by instrumented sharp indentation. Acta Metallurgica **46**, 16, 5755-5767 (1998).

[4] W.C. Oliver, G.M. Pharr, Measurement of hardness and elastic modulus by instrumented indentation: Advances in understanding and refinements to methodology. Journal of Materials Research **19**, 1, 3-20 (2004).

[5] G.M. Pharr, A. Bolshakov, Understanding nanoindentation unloading curves. Journal of Materials Research **17**(10), 2660-2671 (2002).

[6] M. Nishikawa, H. Soyama, Two-step method to evaluate equibiaxial residual stress of metal surface based on micro-indentation tests. Materials and Design **32**, 3240–3247 (2011).